INTERNATIONAL JOURNAL OF INTEGRATED ENGINEERING
ISSN: 2229-838X e-ISSN: 2600-7916

IJIE

Vol. 16 No. 4 (2024) 239-249
https://publisher.uthm.edu.my/ojs/index.php/ijie

The Experimental Analysis and Behaviour of Locally Corroded Metakaolin-Blended Reinforced Concrete Beams Under Flexural Loading

Alamsyah[1, 3], Mohd Hanif Ismail[1], Sallehuddin Shah Ayop[1]*, Francis George Ambros[2]

[1] *Faculty of Civil Engineering and Built Environment, Universiti Tun Hussein Onn Malaysia, 86400 Parit Raja, Johor, MALAYSIA*
[2] *Kinetic Building Technology Sdn Bhd, 47620 Subang Jaya, Selangor, MALAYSIA*
[3] *Department of Civil Engineering, Politeknik Negeri Bengkalis, 28714, Riau, INDONESIA*

*Corresponding Author: sallehs@uthm.edu.my
DOI: https://doi.org/10.30880/ijie.2024.16.04.028

Article Info

Received: 15 May 2024
Accepted: 10 August 2024
Available online: 27 October 2024

Keywords

Accelerated corrosion, flexural strength, metakaolin, resistance sodium chloride

Abstract

The deterioration of reinforced concrete (RC) structures, primarily attributed to the corrosion of reinforcement, is significant in constructions situated in coastal areas. Therefore, this experimental study aimed to evaluate the repercussions of corrosion on the flexural strength of RC beams by introducing Metakaolin (MK) to enhance concrete properties including compressive and flexural strength, as well as resistance to chloride penetration. Accelerated corrosion aging techniques were used to induce 10% corrosion in the reinforcing bars embedded in concrete. The corrosion resistance characteristics of longitudinal bars mixed with 10% MK were scrutinized using a half-cell potential test. The actual extent of corrosion in the tensile reinforcement within the 500 mm beam span was determined by extracting the reinforcing bars from the concrete. The parameters evaluated include flexural strength, load-deflection relationship, and failure modes in both uncorroded and corroded RC beams. The results showed that an enhancement in the flexural strength was observed under four-point bending for RC beams corroded with MK compared to those without MK. Additionally, corrosion-induced pitting on the concrete surface led to spalling mechanisms in the beam. These results underscored the positive influence of incorporating MK into concrete, specifically in beams affected by localized corrosion at mid-span. In general, the addition of MK to the concrete mix provided advantages in terms of flexural strength and durability.

1. Introduction

The corrosion of embedded steel, leading to the deterioration of structures, is recognized as a significant durability challenge encountered by the construction industry [1]. Efforts are continuously being made to address this issue, particularly in enhancing concrete for increased corrosion resistance, one of which entails the addition of fly ash [2]. Moreover, the incorporation of other additives has a positive impact on concrete, for instance, the inclusion of 10% metakaolin (MK) can enhance compressive strength, sequentially providing excellent effects on air and water permeability [3].

The Rapid Chloride Permeability Test (RCPT) serves as a benchmark to determine the resistance level of concrete to the penetration of sodium chloride. [4], [5] conducted a study with the addition of MK and obtained excellent results, specifically achieving a "very low" value in chloride ion penetrability. Several advantages discussed indicated that the use of MK could provide positive values, particularly in corrosion resistance. However, it is essential to consider the percentage of addition because the higher the MK content, the greater the reduction in slump. [6] reported that the use of 10% MK could reduce the slump by up to 61.7% from the normal concrete. The reduction was attributed to the finer particles of MK compared to PC particles, underscoring the higher water demand of MK for the hydration process [7]. However, this slump reduction could still be applied to reinforced structures, provided the slump of normal concrete has been adjusted to about 200 mm.

In general, studies regarding corroded reinforced concrete (RC) beams in laboratories commonly used impressed current on the reinforcement and a stainless plate as the anode and cathode respectively, applying DC voltage through a power source. A vital aspect to consider when accelerating the corrosion process is the density current. In this context, using a high-density current can expedite the occurrence of rust, leading to crack formation and affecting the bonding strength [8]. The use of density current from 50 μA/cm^2 to 300 μA/cm^2 has varying effects on the test specimen, as shown by [9].

Considering the real conditions in the field, where corrosion damage in concrete structures does not immediately occur uniformly across the entire span, it is essential to assess the dominant impact, specifically on the section with the maximum moment in a beam. The percentage of corrosion in the structure also needs attention, as it relates to the maintenance actions for the service life of the structure. A 10% corrosion in the reinforcing steel is more appropriate to consider, as this damage level often signals the initiation of civil engineering maintenance operations [10].

This study aimed to understand the behaviour of RC beams with the addition of MK, particularly the impact of 10% corrosion on the maximum moment of the beam. Normal concrete was designed with a strength of 40 MPa and a slump of 200 mm. Based on previous studies, the addition of MK assumedly produced high-strength concrete (HSC) that fell within the slump specifications commonly used in general RC beam construction, eliminating challenges in compaction. The resulting HSC also offers enhanced resistance to concrete, making it more resilient against sodium chloride attacks. Furthermore, the advantages of the produced concrete offer benefits in the tested characteristics, both corroded and uncorroded beams.

2. Experiment

2.1 Materials and Specimens

The materials used include four reinforced concrete (RC) beams, identified by the codes UB1, CB1, UB2, and CB2. UB1 and CB1 were manufactured using normal concrete, while UB2 and CB2 were produced with 10% metakaolin-blended concrete. The incorporation of 10% MK served as a replacement for 10% of the cement content. Table 1 shows the composition of the mixture for 1 m^3 of normal concrete, grade 40, and concrete with a cement replacement of 10% MK.

Table 1 *Specimens and material mix portion for 1 m^3*

Specimens	Concrete Type	Cement (kg)	Water (kg)	Metakaolin (kg)	Sand (kg)	Coarse Aggregate (kg)	RSS233 (ml)	RF610 (ml)
UB1 CB1	0% MK	500	160		783	957	1980	2640
UB2 CB2	10%MK	450	160	50 kg	783	957	1980	2640

The utilization of superplasticizers (RSS233 and RF610) in this mixture was crucial, considering the transportation process from the factory to the casting site and also for maintaining good workability. The compressive strength of these cubes adhered to British Standard [11], and the data are shown in Table 2. As illustrated in Fig. 1, the beams complied with the intermediate provisions according to the a/d ratio specifications [12]. Positioned on simple supports and spanning 1500 mm, all beams were subjected to four-point bending tests.

The tensile characteristics of uncorroded reinforcement bars were assessed in accordance with the standard [13]. The yield (f_y) and ultimate strength (f_u) of 12 mm diameter tensile reinforcement were determined to be 584.2 MPa and 707.3 MPa, while the values for the 10 mm diameter compression bar were 595.7 MPa and 695.2 MPa respectively. Similarly, for the 8 mm diameter stirrup bar, the yield and ultimate strength were determined to be 561.8 MPa and 600.9 MPa, respectively.

Int. Journal of Integrated Engineering Vol. 16 No. 4 (2024) p. 239-249

Table 2 *Summary of specimens*

Specimens	Concrete Type	Cube Strength (MPa)	Targeted Corrosion (%)	i_{corr} (μA/cm²)	I_{corr} (A)	Surface Area (cm²)	t (h)
UB1	0% MK	48.5					
CB1	0%MK	48.5	10	200	0.0754	376.991	1121.76
UB2	10%MK	58.6					
CB2	10%MK	58.6	10	200	0.0754	376.991	1121.76

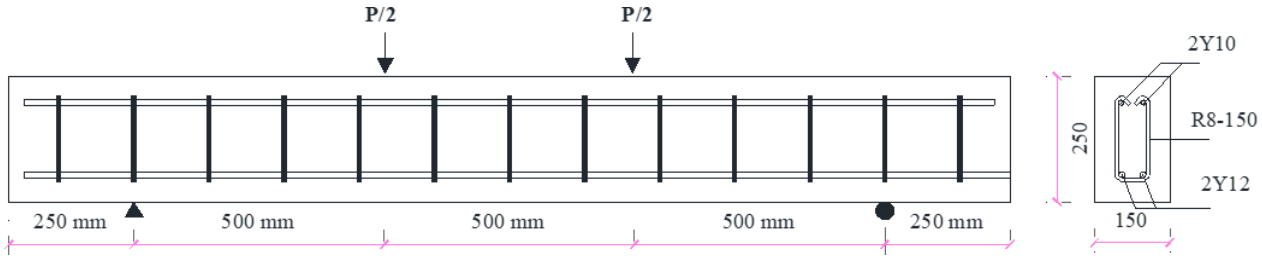

(a)

(b)

Fig. 1 *Beam (a) reinforcement detail; (b) installation of shrink tube on the stirrup*

2.2 Accelerated Corrosion by Impressed Current Method

The acceleration process was carried out by placing the tension side of the beam in the upper position, allowing the tensile bars to be in proximity to the stainless plate. To ensure the continuation of the impressed current process, the stainless section was kept wet using a foam sponge and gunny sack bag. The submersible water pump remained in the position throughout this process to enable 3% NaCl solution flow from the storage tank to the beam, particularly in the central 500 mm section. In this investigation, a current density of 200 μA/cm² was used, in line with the methodology adopted by previous studies [14], [15]. The selection of this particular density was made to replicate conditions encountered in actual environments as well as to avoid adverse effects on the bond between the reinforcement bars and the concrete. [16] showed that when the corrosion current exceeded 200 μA/cm², the width of cracks and strain response intensified significantly. Moreover, the morphology of corrosion products deviated from natural corrosion patterns under high current density conditions.

The corrosion process was implemented on two 12 mm diameter tensile reinforcement bars, each spanning 500 mm at the mid-span. To ensure that the applied current was uniform for both reinforcements, two potentiometers were installed between the Power Supply (PS) and the two reinforcements as anodes. Corrosion was prevented in other reinforcement sections by installing shrink tubes on the stirrup. The time needed to corrode 10% of two 12 mm diameter reinforcement bars, each with a length of 500 mm, was computed using Faraday's law as outlined in Eq. (1). Table 2 showed the duration of electric current application for the corrosion process, while the actual corrosion in steel reinforcement was evaluated by calculating the weight loss, following the procedures outlined in ASTM standards [17].

$$\Delta m = \frac{M.I.\Delta t}{Z.F} \tag{1}$$

where Δm = steel bar weight loss (g), M = atomic mass of Fe (56 g/mol), I = corrosion current (A), Δt = time duration (s), Z = valency of Fe (2), and Faraday constant is 96,500 C/mol.

$$\eta = \frac{m_o - m_c}{m_o} \times 100\% \quad (2)$$

where η = actual corrosion (%); m_0 and m_c are the mass of virgin and corroded steel bars, respectively.

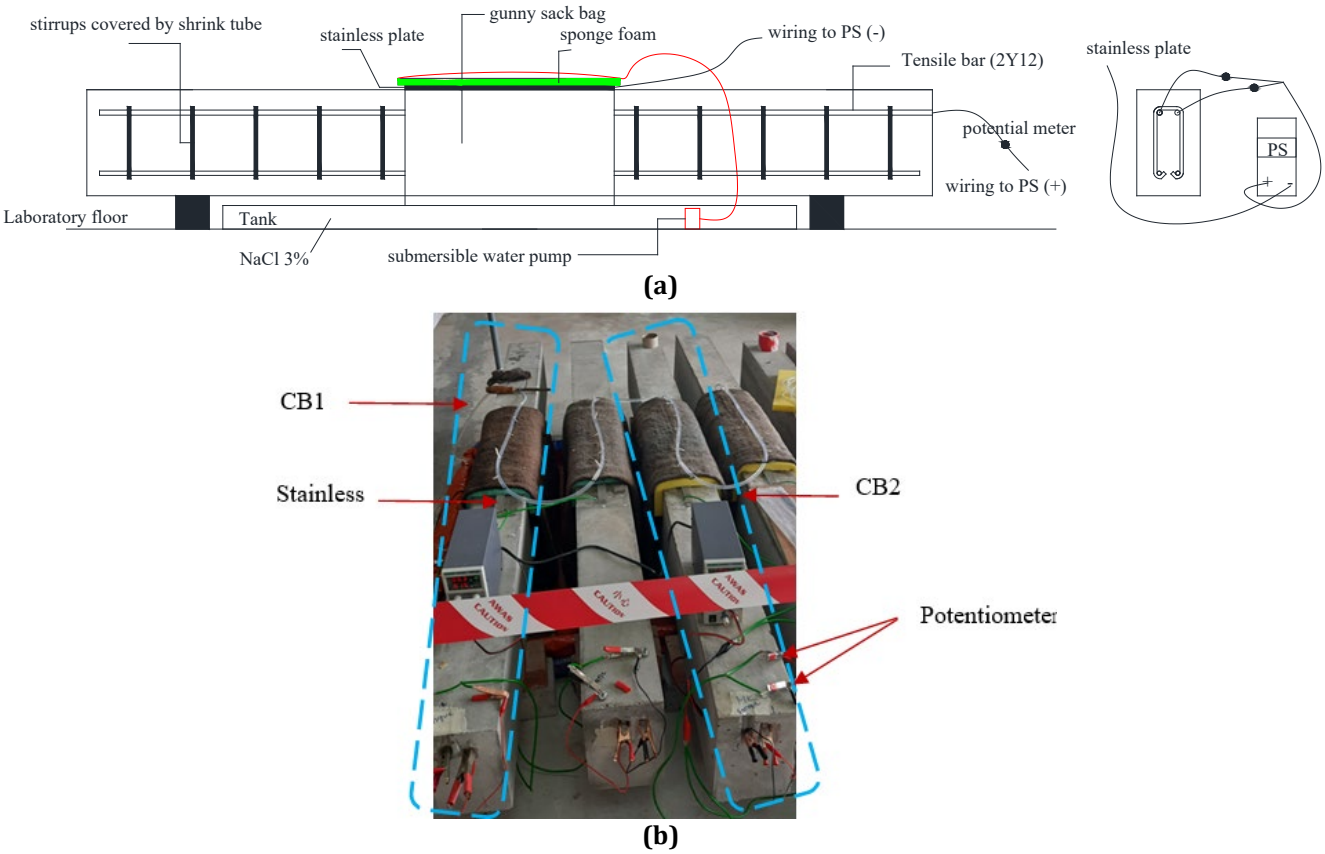

Fig. 2 *Accelerated corrosion (a) detail setting up; and (b) application of accelerated corrosion to test objects*

Due to the 10% corrosion target on CB1 and CB2, two separate power supplies were implemented to control the required electrical current for each test specimen, as depicted in Fig. 2. The conducted procedures indicated the need for different voltages to achieve an electrical current of 0.0754 A, as shown in Fig. 3.

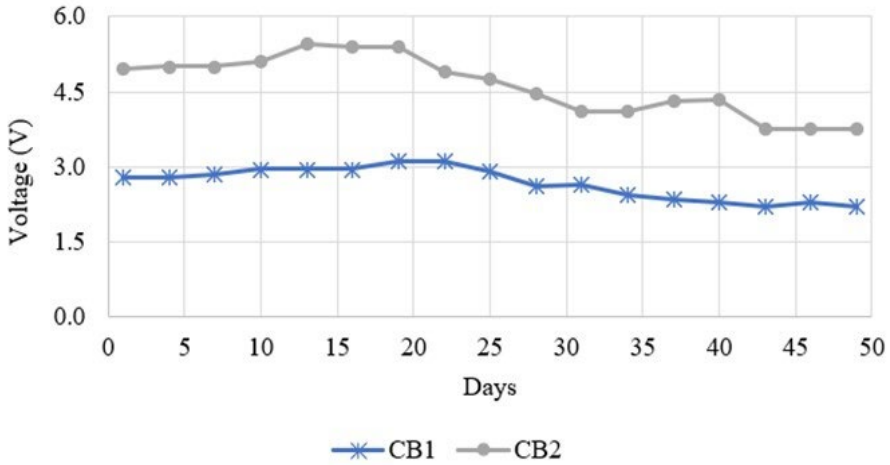

Fig. 3 *The voltage required throughout the process*

Int. Journal of Integrated Engineering Vol. 16 No. 4 (2024) p. 239-249

$$I = \frac{V}{R} \tag{3}$$

where I = corrosion current (A), V = voltage, R = Resistance (Ω).

2.3 Half-Cell Potential Analysis

The probability of corrosion in the embedded reinforcement of RC members was evaluated following the ASTM [18], as shown in Table 3.

Table 3 *Corrosion activity according to half-cell values*

HCP (mV) Cu/CuSO4 (CSE)	Likely Corrosion Condition
> -200	Low (10% risk of corrosion)
-200 to -350	Intermediate corrosion
< -350	High (90% risk of corrosion)
< -500	Severe corrosion

Data for Half-Cell Potential (HCP) were collected at 22 points in the area of 500 mm x 150 mm, specifically on the installed tensile reinforcement, for CB1 and CB2. Fig. 4 shows the data collection process for each beam and the test results are discussed in the subsequent section.

Fig. 4 *HCP data collection*

2.4 Static Loading Test

The flexural test setup and the schematic representation of the RC beam specimen are illustrated in Fig. 5. Two supports were used for the RC beams, and a static piston with a 1000 kN capacity was attached to the loading frame. The distance between the supports was fixed at 1500 mm, resulting in a 250 mm overhang beyond both supports. The beams were subjected to testing until failure, and measurements were recorded for the loads at the initiation of the first cracks, yielding of bars, and ultimate failure. At each incremental load, the deflection at mid-span was measured using an LVDT.

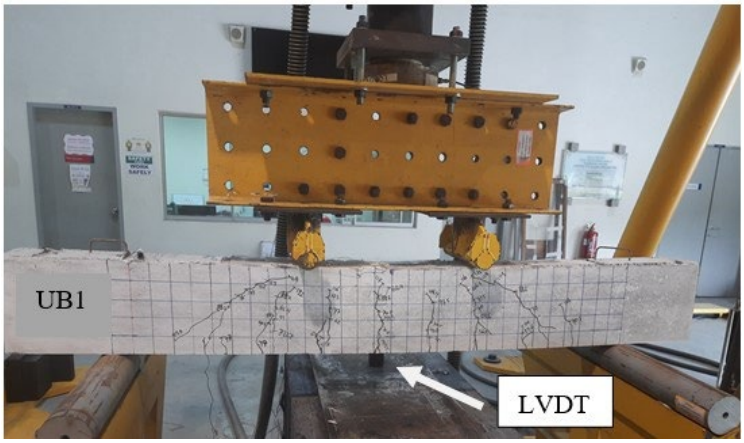

Fig. 5 *Static loading test system*

3. Result and Discussion

3.1 Corrosion and Cracking

According to the calculation of time for 10% corrosion in Table 2, after reaching 1121.76 hours, data collection for HCP was continued as illustrated in Fig. 4.

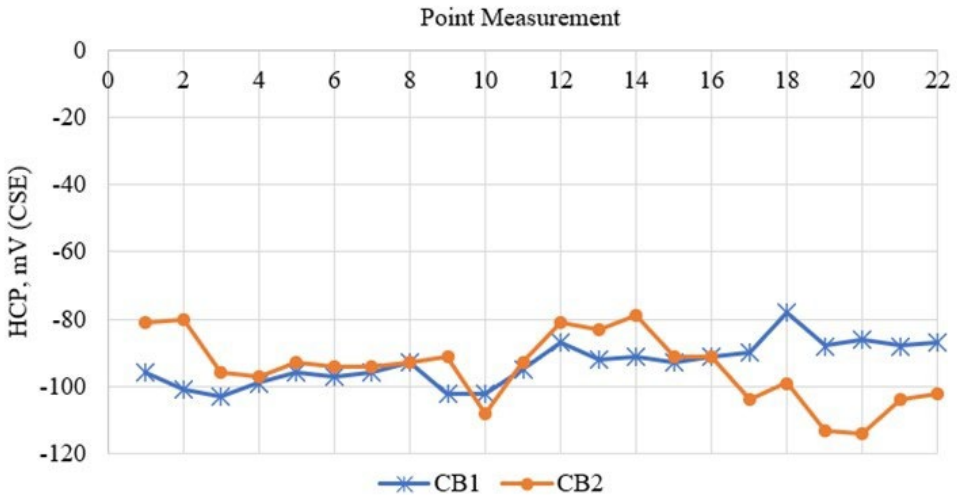

Fig. 6 *Half-cell potential data*

Fig. 6 showed that the measurement results for each beam at 22 points were > -200 mV. Based on Table 3, this suggested the likelihood of corrosion occurring was approximately 10%. However, this method cannot precisely determine the exact percentage. The actual results are presented in the subsequent discussion using the gravimetric method.

(a) **(b)**

Fig. 7 *Corrosion crack (a) CB1 horizontal crack; (b) CB2 horizontal crack*

Int. Journal of Integrated Engineering Vol. 16 No. 4 (2024) p. 239-249

As previously explained, the corrosion process was conducted by placing the tension side of the beam in an upper position. Fig. 7 showed that after reaching 1121.76 hours of the corrosion process, horizontal cracks occurred on the side of the beam. However, there was no significant difference observed, as both test specimens were targeted to corrode by 10%.

3.2 Load-Displacement

The loads, deflections, and strains that occurred were recorded on the data logger, with the first crack load occurring in the test specimen. The results of loads and deflections in the flexural testing are presented in Table 4.

Aside from the increase in concrete compressive strength, the utilization of MK in UB2 also resulted in a 13.1% rise in flexural strength compared to UB1. The localized corrosion on the mid-span reinforcement of CB1 and CB2 reduced the cross-sectional area. Based on the results, there was a 39.7% and 31.4% decrease in strength of CB1 and CB2 compared to UB1 and UB2. This reduction occurred concurrently with the diminished ability of the beam's tension side to withstand tensile forces due to the reduction in the area and the decrease in steel strength after corrosion.

Table 4 *Load and deflection data*

Specimens	P_{cr} (kN)	δ_{cr} (mm)	P_y (kN)	δ_y (mm)	P_u (kN)	δ_u (mm)
UB1	25.55	0.53	90.3	6.25	123.03	20.22
CB1	25.57	0.41			88.04	8.42
UB2	24.75	0.55	91.41	4.64	139.09	13.06
CB2	23.40	0.34			105.87	13.06

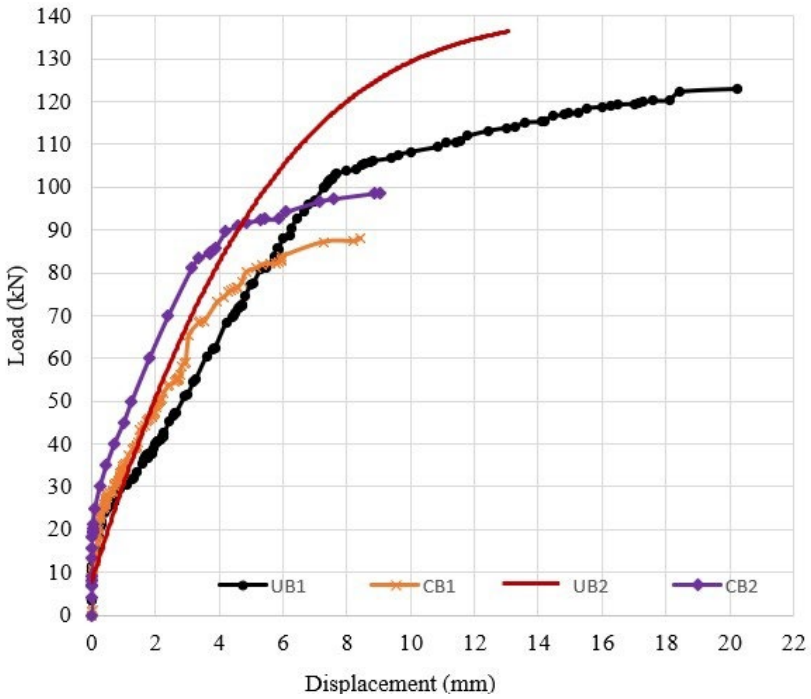

Fig. 8 *Deflection-load diagram*

Fig. 8 showed that corrosion had a negative impact on both normal concrete samples and those blended with metakaolin (MK). However, the decline in strength for the metakaolin-blended concrete was better than that of the normal. Based on the deflection under identical load conditions, the corroded beam had a higher deflection compared to the uncorroded. This observation was consistent with [19] stating that the corrosion of reinforcing bars negatively influenced the deformation corresponding to the ultimate load. The failures observed also fall within the category reported by [20], stating that corrosion above 10% led to brittle failure.

3.3 Failure Mode

In the UB1 and UB2 specimens, an increase in load was accompanied by the addition of flexural cracks in the middle of the beam. Subsequently, there was an increase in shear-flexural cracks as the load continued to increase. In CB1 and CB2, horizontal cracks occurred due to corrosion, and the increase in load was accompanied by flexural-shear cracks (see Fig. 9). The increase in load caused the enlargement of corrosion cracks, leading to spalling, specifically for corroded specimens.

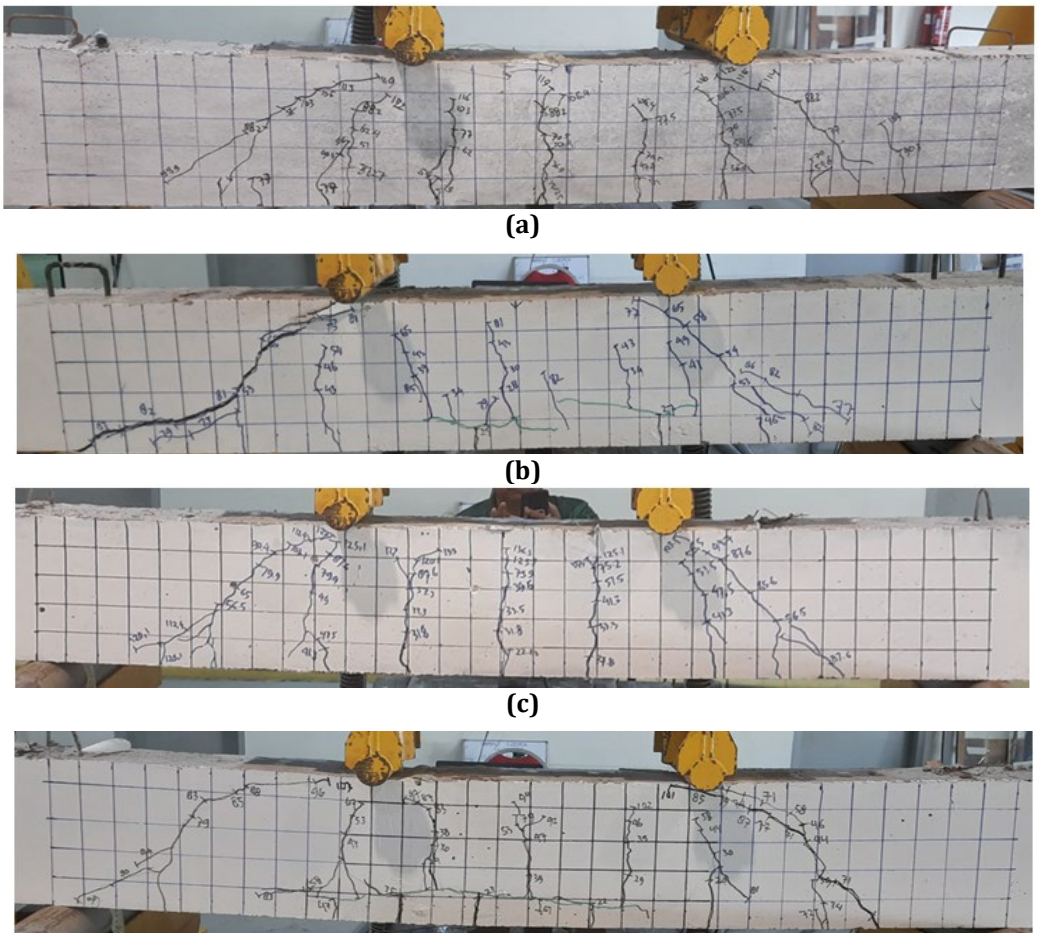

(a) **(b)** **(c)** **(d)**

Fig. 9 *Crack pattern of specimens (a) UB1; (b) CB1; (c) UB2; (d) CB2*

The uncorroded specimens were designed to possess higher shear resistance than flexural to induce failure. This phenomenon was observed in UB1 and UB2, despite the crack pattern being categorized as flexural-shear. A different scenario was evident in the corroded test specimens, where more dominant shear cracks were observed toward the support, specifically in CB1. This occurred due to changes in the bond of the reinforcement and strains, contributing to differences in the equilibrium of forces and compatibility of RC beam deformations [21], as shown in Fig. 10.

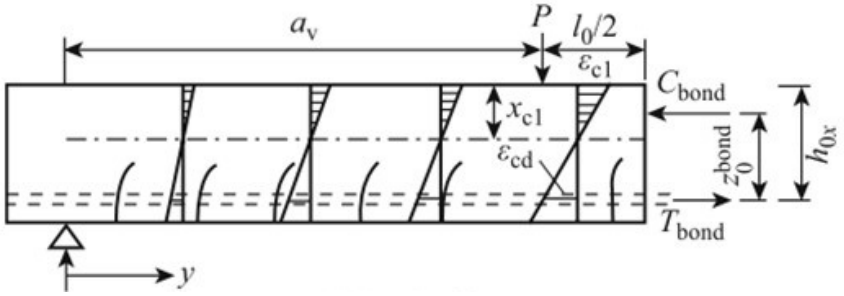

(a)

Int. Journal of Integrated Engineering Vol. 16 No. 4 (2024) p. 239-249

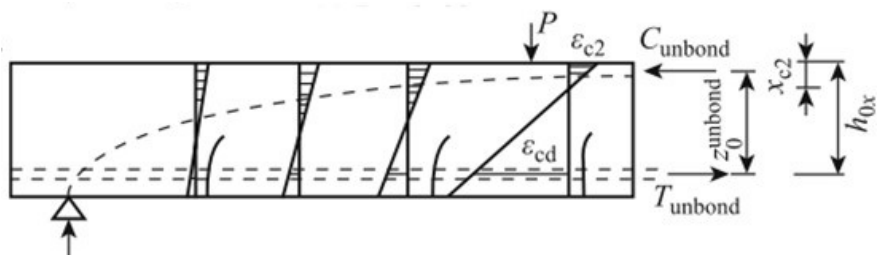

(b)

Fig. 10 *Equilibrium of forces and compatibility of deformations (a) bonded beam; (b) unbonded beam*

3.4 Corroded Steel Bar After Testing

After completing the flexural testing phase, the corroded reinforcing steel was retrieved and cleaned using a 12% hydrochloric acid solution. The steel was rinsed with distilled water, dried, and weighed, while the results of weight measurement were calculated using Eq. (2), resulting in actual corrosion values of 6.51% and 7.86% for CB1 and CB2, respectively. These results indicate values below the target of 10%, as also reported in similar studies by [10], [14], [22]. The corrosion observed was not only confined to the 500 mm at the mid-span but also spread approximately 50 mm to other areas (see Fig. 11). This could be due to the absorption and wetting of the reinforcement by the sodium chloride flow outside the targeted area.

The reinforcing steel, which had been cleaned of rust, was subjected to a tensile test and the results obtained were presented in Table 5. The reduction in stress within the rusted steel was due to changes in cross-sectional area, as well as the presence of pits. According to [15], corrosion pits, similar to mechanical notches on the surface of steel reinforcement bars, tend to intensify local stress fields. This diminished the performance of the bar as reinforcement in reinforced concrete (RC) beams.

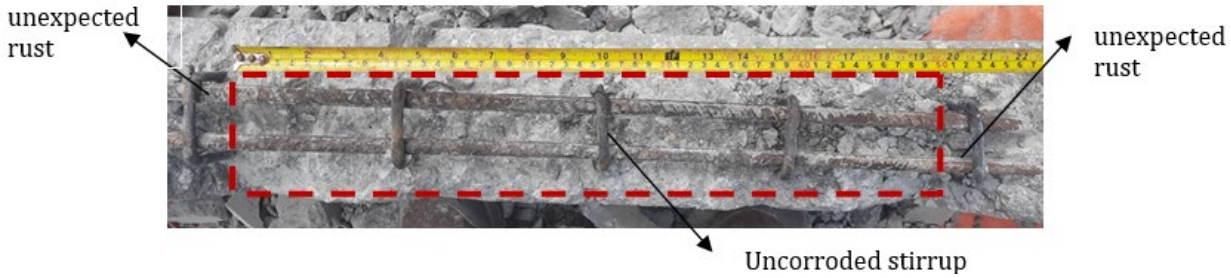

Fig. 11 *Rust on tensile reinforcement*

Table 5 *Tensile data of tensile bar*

Specimens	Uncorroded bar		Corroded bar	
	f_y	f_u	f_y	f_u
CB1	584.2	707.3	462.5	537.5
CB2	584.2	707.3	528.5	571.5

4. Conclusion

In conclusion, corrosion of reinforcement poses a significant threat to the long-term durability of reinforced concrete (RC) structures globally. Based on the results, corrosion in the RC led to the expansion of rust and a reduction in the cross-sectional area of the reinforcing bars, ultimately causing concrete cracking in structural elements. A comprehensive review of the existing literature showed that issues related to expansion could be addressed by protecting steel reinforcing bars from corrosion or using additional materials capable of inhibiting corrosion. However, existing studies have not extensively explored the response of corroded RC beams containing Metakaolin (MK) under flexural loading. To address this gap, this experimental study was conducted to assess the impact of corrosion on the flexural capacity of RC beams with MK used as a strength enhancer and corrosion inhibitor. The conclusions drawn from the results are as follows:

- Incorporating MK resulted in an enhancement of both compressive and flexural strength in concrete.
- The incorporation of MK in concrete beams improved the quality of the concrete, rendering it more resistant to sodium chloride penetration.
- The degradation of beams due to corrosion indicated that beams with MK perform better than normal ones.

- Corroded beams experienced spalling in the concrete cover, both in CB1 and CB2.

Acknowledgement

This study received support from the Ministry of Higher Education (MOHE) through the Fundamental Research Grant Scheme (FRGS/1/2021/STG05/UTHM/03/2). The authors are grateful to Politeknik Negeri Bengkalis, as well as the staff of the Laboratory and the Jamilus Research Centre for Sustainable Construction (JRC-SC) in the Faculty of Civil Engineering and Built Environment at Universiti Tun Hussein Onn Malaysia.

Conflict of Interest

Authors declare that there is no conflict of interests regarding the publication of the paper.

Author Contribution

The authors confirm contribution to the paper as follows: ***study conception and design:*** *Alamsyah, Sallehuddin Shah Ayop, Mohd Hanif Ismail;* ***data collection:*** *Alamsyah;* ***analysis and interpretation of results:*** *Alamsyah, Mohd Hanif Ismail, Sallehuddin Shah Ayop, Francis George Ambros;* ***draft manuscript preparation:*** *Alamsyah. Sallehuddin Shah Ayop. All authors reviewed the results and approved the final version of the manuscript.*

References

[1] Li, C., Chen, Q., Wang, R., Wu, M., & Jiang, Z. (2020). Corrosion assessment of reinforced concrete structures exposed to chloride environments in underground tunnels: Theoretical insights and practical data interpretations. Cement and Concrete Composites, 112, 103652. https://doi.org/10.1016/j.cemconcomp.2020.103652

[2] Sathe, S., & Patil, S. (2023). Experimental analysis and behavior of corrosion-damaged fly ash blended reinforced concrete beam under flexural loading. Journal of Building Pathology and Rehabilitation, 8(2), 1–17. https://doi.org/10.1007/s41024-023-00344-9

[3] Pillay, D. L., Olalusi, O. B., Kiliswa, M. W., Awoyera, P. O., Kolawole, J. T., & Babafemi, A. J. (2022). Engineering performance of metakaolin-based concrete. Cleaner Engineering and Technology, 6, 100383. https://doi.org/10.1016/j.clet.2021.100383

[4] Shafiq, N., Kumar, R., Zahid, M., & Tufail, R. F. (2019). Effects of modified metakaolin using nano-silica on the mechanical properties and durability of concrete. Materials, 12(14), 1–22. https://doi.org/10.3390/ma12142291

[5] Sharobim, K. (2021). Prediction of service life of structures contain metakaolin concrete. International Journal of Engineering Sciences & Research Technology, 10(2), 19–30. https://doi.org/10.29121/ijesrt.v10.i2.2021.3

[6] Ismail, M. H., Megat Johari, M. A., Ariffin, K. S., Jaya, R. P., Wan Ibrahim, M. H., & Yugashini, Y. (2022). Performance of high strength concrete containing palm oil fuel ash and metakaolin as cement replacement material. Advances in Civil Engineering, 2022(2), 1-11. https://doi.org/10.1155/2022/6454789

[7] Pillay, D. L., Olalusi, O. B., Awoyera, P. O., Rondon, C., Echeverría, A. M., & Kolawole, J. T. (2020). A Review of the engineering properties of metakaolin based concrete: Towards combatting chloride attack in coastal/marine structures. Advances in Civil Engineering, 2020, 1-13. https://doi.org/10.1155/2020/8880974

[8] Ayop, S. S., & Cairns, J. J. (2015). The Influence of impressed current on residual bond strength of corroded structure. Applied Mechanics and Materials, 773–774, 984–989. https://doi.org/10.4028/www.scientific.net/amm.773-774.984

[9] Zhang, W., Chen, J., & Luo, X. (2019). Effects of impressed current density on corrosion-induced cracking of concrete cover. Construction and Building Materials, 204, 213–223. https://doi.org/10.1016/j.conbuildmat.2019.01.230

[10] Lejouad, C., Richard, B., Mongabure, P., Capdevielle, S., & Ragueneau, F. (2022). Experimental study of corroded RC beams: Dissipation and equivalent viscous damping ratio identification. Materials and Structures/Materiaux et Constructions, 55(2), 73. https://doi.org/10.1617/s11527-022-01906-y

[11] BS EN 12390-3 (2002). Testing Hardened Concrete - Part 3: Compressive Strength of Test Specimens. BSI Standards.

[12] Wang, C. K., Salmon, C. G., Pincheira, J. A. (2007). Reinforced Concrete Design. Jhon Wiley and Sons.

[13] BS EN ISO 6892 (2019). Metallic Materials - Tensile Testing. BSI Standards.

[14] Li, Q., Jin, X., Yan, D., Fu, C., & Xu, J. (2021). Study of wiring method on accelerated corrosion of steel bars in concrete. Construction and Building Materials, 269, 121286. https://doi.org/10.1016/j.conbuildmat.2020.121286

[15] Song, L., Fan, Z., & Hou, J. (2019). Experimental and analytical investigation of the fatigue flexural behavior

of corroded reinforced concrete beams. International Journal of Concrete Structures and Materials, 13 (24), 1-14. https://doi.org/10.1186/s40069-019-0340-5

[16] El Maaddawy, T. A., & Soudki, K. A. (2003). Effectiveness of impressed current technique to stimulate corrosion of steel reinforcement in concrete. *Journal of Materials in Civil Engineering, 15(1),41-47.* https://doi 10.1061_(ASCE)0899-1561(2003)15_1(41).

[17] ASTM G1-90 (1999). Standard practice for preparing, cleaning, and evaluating corrosion test. Significance, 90, 1–9. https://doi.org/10.1520/G0001-03.2

[18] ASTM C876-15. (2017). Standard Test Method for Corrosion Potentials of Uncoated Reinforcing Steel. Standard Test Method for Corrosion Potentials of Uncoated Reinforcing Steel in Concrete, pp. 1–8.

[19] Jung, J. S., Lee, B. Y., & Lee, K. S. (2019). Experimental Study on the structural performance degradation of corrosion-damaged reinforced concrete beams. Advances in Civil Engineering, 2019, 1-14. https://doi.org/10.1155/2019/9562574

[20] Tamai, H., Sonoda, Y., & Bolander, J. E. (2020). Impact resistance of RC beams with reinforcement corrosion: Experimental observations. Construction and Building Materials, 263, 120638. https://doi.org/10.1016/j.conbuildmat.2020.120638

[21] Wang, X. H., & Liu, X. L. (2008). Modeling the flexural carrying capacity of corroded RC beam. Journal of Shanghai Jiaotong University (Science), 13, 129–135. https://doi.org/10.1007/s12204-008-0129-1

[22] Di Carlo F., Meda A & Rinaldi Z. (2023). Structural performance of corroded RC Beam. Engineering Structures, 274, 115117. https://doi.org/10.1016/j.engstruct.2012.115117